ONCOIMMUNOLOGY
2025, VOL. 14, NO. 1, 2455176
https://doi.org/10.1080/2162402X.2025.2455176

Taylor & Francis
Taylor & Francis Group

ORIGINAL RESEARCH

OPEN ACCESS Check for updates

Liver metastases of colorectal cancer contain different subsets of tissue-resident memory CD8 T cells correlated with a distinct risk of relapse following surgery

Syrine Abdeljaoued[a,b], Alexandre Doussot[c], Marie Kroemer[a,b,d], Emilien Laloy[a], Jean René Pallandre[a], Antoine El Kaddissi[a,e], Laurie Spehner[a,b], Myriam Ben Khelil[a], Adeline Bouard[a,f], Virginie Mougey[a,f], Ugo Chartral[a], Angélique Vienot[a,b,e], Julien Viot[a,b,e], Zaher Lakkis[a,c], Franck Monnien[a,g], Romain Loyon[a], and Christophe Borg[a,b,e]

[a]Université de Franche-Comté, EFS, INSERM, UMR RIGHT, Besançon, France; [b]Clinical Investigational Center, France; [c]Department of Digestive and Oncologic Surgery, Liver Transplantation Unit, University Hospital of Besançon, Besançon, France; [d]Department of Pharmacy, University Hospital of Besançon, Besançon, France; [e]Department of Medical Oncology, University Hospital of Besançon, Besançon, France; [f]ITAC platform, University of Bourgogne Franche-Comté, Besançon, France; [g]Department of Pathology, University Hospital of Besançon, Besançon, France

ABSTRACT

Tissue-resident memory (T_{RM}) T cells have emerged as key players in cancer immunosurveillance, and their presence has been linked to a favorable clinical outcome in solid cancer patients. Liver metastases exhibit a highly immunosuppressive tumor microenvironment, however, the role and clinical impact of T_{RM} cell infiltration in colorectal cancer remain elusive. The expression of several tissue residency and activation biomarkers has been investigated on tumor-infiltrating lymphocytes isolated from 26 patients' colorectal cancer liver metastases (CRC liver metastases) and compared to 16 peripheral blood samples of patients with CRC liver metastases. Cytokine production was also evaluated in *in vitro-activated* T_{RM} and non-T_{RM} cells. The prognostic value of T_{RM} cells was also assessed in a well-defined cohort of CRC liver metastases. Here we identified two subsets of T_{RM} cells expressing CD103 and/or CD69 showing significantly higher expression of tissue residency and activation biomarkers. $CD103^+CD69^+$ T_{RM} cells subset showed almost exclusive expression of tumor reactivity biomarkers PD-1 and CD39. Supporting this observation, $CD103^+CD69^+$ T_{RM} cells showed a more oligoclonal TCR repertoire. Both T_{RM} subsets presented higher cytotoxic and functional capacity compared to non-T_{RM} cells. Our study shows that only the presence of $CD103^+CD69^+$ T_{RM} cells is associated with longer recurrence-free survival of colorectal cancer patients with liver metastases. Taken together, our work demonstrates the existence of a phenotypic heterogeneity of T_{RM} cells in colorectal cancer liver metastases. In this study, we identified a population of $CD103^+CD69^+$ T_{RM} cells exhibiting the characteristics of tumor reactivity and correlated with better patients' prognosis, with potential implications in optimal therapeutic strategies determination.

ARTICLE HISTORY
Received 18 September 2024
Revised 13 January 2025
Accepted 14 January 2025

KEYWORDS
Colorectal cancer; liver metastases; prognosis; Tissue-resident memory t cells; T_{RM}

CONTACT Syrine Abdeljaoued abdeljaoued.syrine@hotmail.fr; Christophe Borg christophe.borg@univ-fcomte.fr Université de Franche-Comté, EFS, INSERM, UMR RIGHT, 8 Rue DU DR JFX Girod, Besançon, 25020 France

Supplemental data for this article can be accessed online at https://doi.org/10.1080/2162402X.2025.2455176

© 2025 The Author(s). Published with license by Taylor & Francis Group, LLC.
This is an Open Access article distributed under the terms of the Creative Commons Attribution-NonCommercial License (http://creativecommons.org/licenses/by-nc/4.0/), which permits unrestricted non-commercial use, distribution, and reproduction in any medium, provided the original work is properly cited. The terms on which this article has been published allow the posting of the Accepted Manuscript in a repository by the author(s) or with their consent.

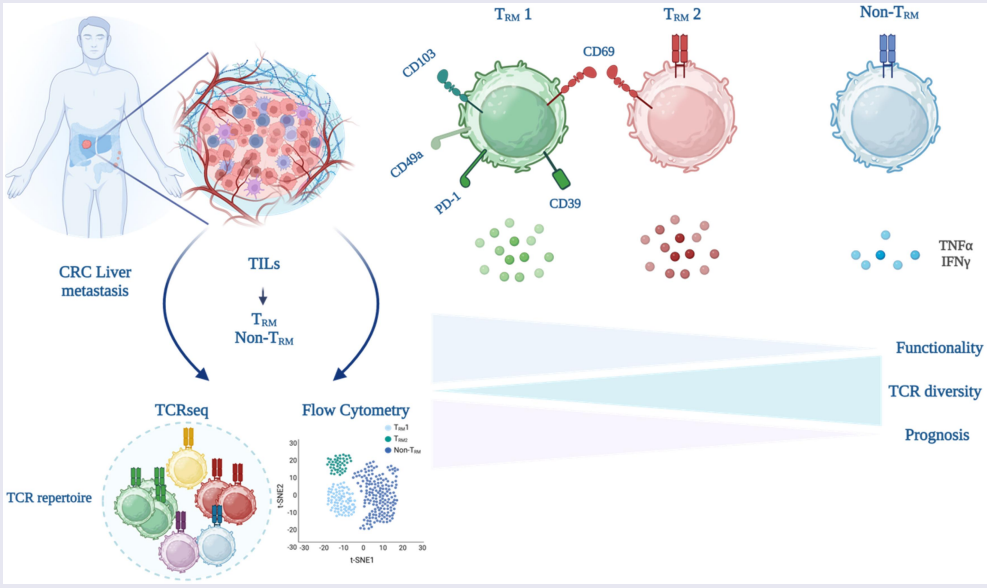

HIGHLIGHTS

- Liver metastases of colorectal carcinoma contain CD103$^+$ CD69$^+$ and CD103$^-$ CD69$^+$ T_{RM} subsets
- CD103$^+$ CD69$^+$ T_{RM} subset is enriched in antigen-experienced lymphocytes expressing PD1 and CD39
- The presence of CD103$^+$CD69$^+$ T_{RM} cells is associated with longer recurrence free survival.

Introduction

Tissue-resident memory T (T_{RM}) cells reside in peripheral tissues where they play a key role in local immunosurveillance and in controlling early pathogen spread.[1] T_{RM} have recently emerged as an essential component in cancer immunity.[2,3] Compelling evidence established that CD8$^+$ T_{RM} cells are endowed for accumulation in the cancer microenvironment, enriched in tumor antigen-specific clones, and display potent and durable effector functions.[4] If the role of T_{RM} cells has been unraveled in primary tumors of epithelial origin, the contribution of these lymphocytes in the immune context of liver metastases is still unclear.

T_{RM} cells have been described within most organs in mice and human and are characterized by the high expression of surface molecules that enforce a tissue-resident state such as CD103, CD69, and CD49a.[2,5] CD103 is the subunit of the Integrin αE that pairs with the subunit of the integrin β7 to form a heterodimeric receptor that binds to E-cadherin and enables tissue retention of T cells.[6,7] CD69 is a type II C-lectin that counteracts tissue egress by down-regulating the expression of sphingosine-1-phosphate receptor-1 (S1PR1).[8,9] CD49a is the Integrin α1 subunit that pairs with the integrin β7 subunit to constitute the VLA-1 (Very Late Antigen 1) which binds to collagen IV.[10]

Even though T_{RM} cells share a common core residency transcriptional program, they have been shown to present inter and intra-organ heterogeneity.[11,12] In recent years, T_{RM} cells transcriptional and functional characteristics have been extensively investigated in the most immunogenic solid cancers such as melanoma and lung cancers, and more recently in breast cancers, however, they remain poorly explored in gastrointestinal cancers.[11,13–17] Interestingly, these studies reported a superior functionality of T_{RM} cells compared to non-T_{RM} cells which may explain the observed correlation of their presence with a better patient outcome at the clinical level. However, the impact of T_{RM} cells subsets presence on the prognosis of cancer patients with liver metastases remains dismal.

Comprehensive analysis of tumor-associated antigens and neoantigens-specific tumor-infiltrating T cells in respectively HBV induced cancers and non-small cell lung cancers at the single cell level revealed that most of these tumor-infiltrating lymphocytes are T_{RM} cells.[18,19] These observations highlight the pivotal role played by T_{RM} cells in cancer eradication and explain their superior prognostic value compared to non-T_{RM} cells.[20]

Liver metastases occur in nearly 50% of patients with colorectal cancer (CRC) and represent the leading cause of CRC-related death.[21] Although curative resection of metastases markedly improves patients' long-term survival, still 70% of these patients relapsed. A comprehensive study conducted on over 200 patients with CRC liver metastases reported that high CD3$^+$ CD8$^+$ TILs density in the tumor microenvironment is associated with better outcome for these patients.[22] A better characterization of T_{RM} distribution and biology within liver metastases might contribute to a better understanding of these diseases.

In this study, we sought to characterize T_{RM} cells populations in colorectal cancer liver metastases for the first time and to investigate their functionality. Therefore, we performed exhaustive phenotypic and functional characterization of TILs of patients with CRC liver metastases using multiparametric flow cytometry and *in vitro* experiments. The prognostic value of these subsets was also assessed in a well-defined cohort of CRC patients who underwent curative surgery for their liver metastases.

Materials and methods

Human subjects

A total of 26 Colorectal cancer liver metastases samples were obtained from the University Hospital of Besançon, Department of Digestive Surgery. Patients with histologically confirmed liver metastases were enrolled in the Epitopes-CRC02 cohort (NCT02817178). Informed consent was obtained from all patients following the French regulations. This study was approved by the local and national ethics committees. Formalin-fixed paraffin-embedded (FFPE) tissue specimens of liver metastases of CRC patients were retrieved from the pathology archives and processed/archived in the Biobank BB-0033-00024, of the Tumorothèque Régionale de Franche-Comté, Project (#F1820).

Tumor-infiltrating lymphocytes and peripheral blood mononuclear cells isolation

Tumor-infiltrating lymphocytes (TILs) were obtained from freshly extracted colorectal cancer liver metastases as previously described. Briefly, tumors were cut and digested using a mechanical/enzymatic dissociation system (Miltenyi Biotec) and then filtered. Flow cytometry staining and functional testing as well as TCR sequencing were conducted on the freshly obtained or cryopreserved cell suspension.

Peripheral blood mononuclear cells (PBMCs) were isolated from blood samples of patients with CRC liver metastases using density gradient centrifugation.

Flow cytometry

Phenotypic analysis of TILs and PBMCs was realized in FACS buffer (PBS 1X, EDTA 50 µM, 0.2% BSA). For surface antigen staining, cells were incubated with the appropriate fluorescence-conjugated antibodies for 30 min in the dark at 4°C (Table S1). For cell viability analyses, fixable viability dye (eBioscience) was used according to the manufacturer's instructions. For intracellular staining, cells were washed after surface antigen staining then permeabilized and fixed using the Fixation/Permeabilization Kit (BD Biosciences) according to the manufacturer's instructions. Finally, cells were stained with the appropriate fluorescence-conjugated antibodies for 30 min in the dark at 4°C. Flow cytometry data were acquired on FACSLyric (BD Biosciences) and analyzed with FlowJo software (v10.8.1). The gating strategy was set on Fluorescence Minus One (FMO) control applied across all samples. Visualization of flow cytometry data using t-SNE or UMAP was achieved using FlowJo software (v10.8.1).

Functional assays

For the assessment of cytokine production and degranulation by T_{RM} and non-T_{RM} cells, TILs were stimulated for 5 h in a plate-bound anti-CD3 (Miltenyi Biotec MACS GMP, clone OKT3) and a soluble anti-CD28 (Miltenyi Biotec, clone 15E8) in the presence of GolgiPlug or GolgiStop (BD Biosciences) in RPMI medium (Thermo Fisher Scientific) supplemented with 10% fetal bovine serum. Coting of the anti-CD3 (2 µg/ml) was performed overnight at 4°C with PBS. After stimulation, intracellular cytokine staining was performed and IFNγ, TNFα, GZMß, and CD107a (BD Biosciences, clone Mab11) (Table S1) were assessed.

TCRα and TCRβ sequencing and analysis

Non-expanded tumor-infiltrating lymphocytes extracted from liver metastasis of CRC were stained with anti-CD3, anti-CD8, anti-CD69, and anti-CD103 antibodies as well as viability dye (Supplementary Table S1). Three $CD8^+$ T cell populations were sorted: two T_{RM} populations identified as $CD69^+CD103^-$ and $CD69^+CD103^+$ as well as a non-T_{RM} population identified as $CD69^-CD103^-$ was used as a control.

Bulk TCR sequencing analyses were performed as described previously.[23] Briefly, RNA was isolated and amplified by *in vitro* transcription. The resulting cRNA was converted to ssDNA by multiplex reverse transcription using a collection of TRAV/TRBV-specific primers containing UMI and Illumina adapters. TCRs were then amplified by PCR (20 cycles) with a single primer pair binding to the constant region and the Illumina adapter added during the reverse transcription. A second round of PCR (25 cycles) was performed to add the different indexes used for multiplexing. The TCR products were purified, quantified, and loaded on MiSeq or NextSeq instruments (Illumina) for the deep sequencing of the TCRs chain. The TCR sequences were further processed using *ad hoc* Perl scripts to (i) pool all TCR sequences coding for the same protein sequence; (ii) correct for amplification and sequencing errors using 9mers UMI; (iii) filter out all out-frame sequences; (iv) determine the abundance of each distinct TCR sequence. TCRs with a single read were removed for the analysis.

Divers indexes such are richness, Shannon Entropy, and clonality were used to analyze the repertoire. Richness refers to the number of unique clonotypes identified in the repertoire. The Shannon Entropy was calculated as follows:

$$-\sum_{i=1}^{n} F_i * log2(F_i)$$

Where n is the total number of clonotype and F is the clonotype frequency. Clonality, refers to 1-Pielou index, was calculated as follows:

$$1 - \left(\frac{-\sum_{i=1}^{n} F_i * log10(F_i)}{log10(n)}\right)$$

Where n is the total number of clonotypes and F is the clonotype frequency.

RNA sequencing analysis

Frozen samples of CRC liver metastases were used for mRNA extraction using Qiagen Kit Qiagen AllPrep DNA/RNA Mini Kit (ref 80,204) as previously described.[24] The concentration of each library was measured by real-time PCR. Samples with a RIN score strictly inferior to 7 were discarded. The constructed libraries were sequenced in paired ends (200 cycles; 2 × 100 bp) using Novaseq 6000.

Local bulk RNA-seq reads were aligned using STAR v2.7.9a to GENCODE Human Release 39 (GRCh38.p13), and the read count matrix was produced with Feature Counts v2.0.1, both by using the default parameters. Immune deconvolution analyses of the datasets were performed using the immunedeconv R package and MCPCounter as previously described.[24] Clustering of the T_{RM}^{high} and T_{RM}^{Low} expression populations was performed by cutting off the median of full CD3, CD8, CD103, and CD69 gene expression for the dataset. Computations were performed at the supercomputer facilities of Mésocenter de calcul de Franche-Comté. Raw data from the bulk RNA-seq analysis were deposited in NCBI Gene Expression Omnibus (GEO) under accession number GSE207194.

Single cell RNA and TCR sequencing data processing

Single cell RNA and TCR sequencing were downloaded from Gene Expression Omnibus (GEO) with the accession number GSE164522.[25] The counts data corresponding to the PBMCs, primary tumor and tumor metastasis were analyzed using Seurat V5.0.0,[26] and the TCR sequencing data was added to the Seurat object using scRepertoire V1.12.0.[27] The quality control was already performed on the downloaded data and no additional filtering was applied. A normalization step was used with the "Log.Normalize" method and with scale factor of 10 000. The scaling step was performed on all genes, and a PCA was runned on the first 2 000 variable genes. Clustering was obtained by finding the closest neighbors by running the Louvain algorithm on the first 30 PC, and at a resolution of 1 by which the CD3E+ CD8A+ cells were clustered separately. After running the UMAP using the same first 30 PC, the Seurat was subseted of clusters that expressed both CD3E and CD8A. The same analysis was performed on the resulted Seurat object, and the resolution of 0.4 was chosen for further analysis. The differentially expressed gene were calculated for each cluster using FindAllMarkers with logfc.threshold = 0.5, min.pct = 0.1 and using the Wilcoxon test. scRepertoire was used to make the figures for scTCR seq data.

Immunohistochemistry and immunofluorescence staining

For CD3 immunohistochemistry, FFPE specimens of CRC liver metastases were sectioned at 4/5 µm. Hematoxylin and eosin staining was performed for the first section to histopathologically confirm the presence of tumor cells. Immunostaining for CD3 with a polyclonal rabbit anti-human CD3 antibody (A045201, Agilent) (1/200) was performed using a Ventana Benchmark (Roche) as previously described in.[24] The CD3 slides were digitized with a Nanozoomer HT2.0 (Hamma- Matsu) at (20×) magnification to generate a whole-slide imaging (WSI) file in ndpi format that was then imported into QuPath software to evaluate densities (cells/mm^2) at the tumor center and the invasion margins of CRC liver metastases. For T_{RM} immunofluorescence staining, the following antibodies were used on 52 CRC liver metastases tissue microarray (TMA): Mouse anti-CD8 (BioSB, BSB 5173) at 1/100 and Rabbit anti-CD103 (Abcam, ab129202) at 1/100. For each staining, a secondary conjugated antibody from Jackson Immunoresearch was used at 1/300: Cy5 Goat anti-mouse (115-175-205), FITC Goat anti-rabbit (111-095-144), AF594 Goat anti-mouse IgG2a (115-585-206). Immunohistochemical and immunofluorescence analyses were performed by an experienced pathologist blinded to patient identity and clinical status.

Statistical analysis

Statistical significance between three or more paired groups was assessed using one-way ANOVA with Tukey's multiple comparisons test. The significance between the two groups was calculated using the Mann-Whitney U test.

Recurrence-free survival (RFS) was calculated from the date of surgery for CRC liver metastases to the date of relapse or death from any cause or to the date of the last follow-up, at which point the data were censored. Overall survival (OS) was calculated from the date of CRC liver metastases surgery to the date of death from any cause. Survival data were censored at the last follow-up visit. OS curves were estimated using the Kaplan-Meier method and described using the median or rate at specific time points with 95% confidence intervals (95%CI).

Analyses and graphical plotting were performed using R software (version 3.6.1; R Development Core Team; http://www.r-project.org) and GraphPad Prism 9. Statistical significance was set at $p < 0.05$.

Data availability statement

Raw data from the bulk RNA-seq analysis were deposited in NCBI Gene Expression Omnibus (GEO) under accession number GSE207194. Raw data are available upon reasonable request from the corresponding author.

Results

CRC liver metastases CD8$^+$ T cells are enriched for tissue residency biomarkers

Multi-parametric flow cytometry profiling was conducted on TILs isolated from 19 patients' colorectal cancer liver metastases and compared to 16 PBMCs samples of CRC liver metastases patients (Figure 1a). Tissue residency, activation, exhaustion as well as tumor reactivity biomarkers were assessed. Analysis revealed a remarkably distinct phenotype of liver metastases CD8$^+$ TILs compared to circulating T cells (Figure 1b,c). CRC liver metastases CD8$^+$ TILs exhibited significantly higher expression of tissue retention biomarkers CD69, CD103, and CXCR6 whereas circulating CD8$^+$ T cells showed no expression of these proteins (Figure 1b,c). CXCR6 and CD101 were reported to be a tissue residency biomarker of liver T_{RM}[28] cells, interestingly while roughly a median of 10% of circulating CD8$^+$ T cells expressed CD101, almost 40% of CD8$^+$ TILs were positive (Figure 1b,c). In addition, we noted that CRC liver metastases CD8$^+$ TILs expressed higher levels of CD39 and PD-1 along with the activation marker HLA-DR (Figure 1b,c). Strikingly, a significant downregulation of the co-stimulation biomarker CD226 was observed in liver

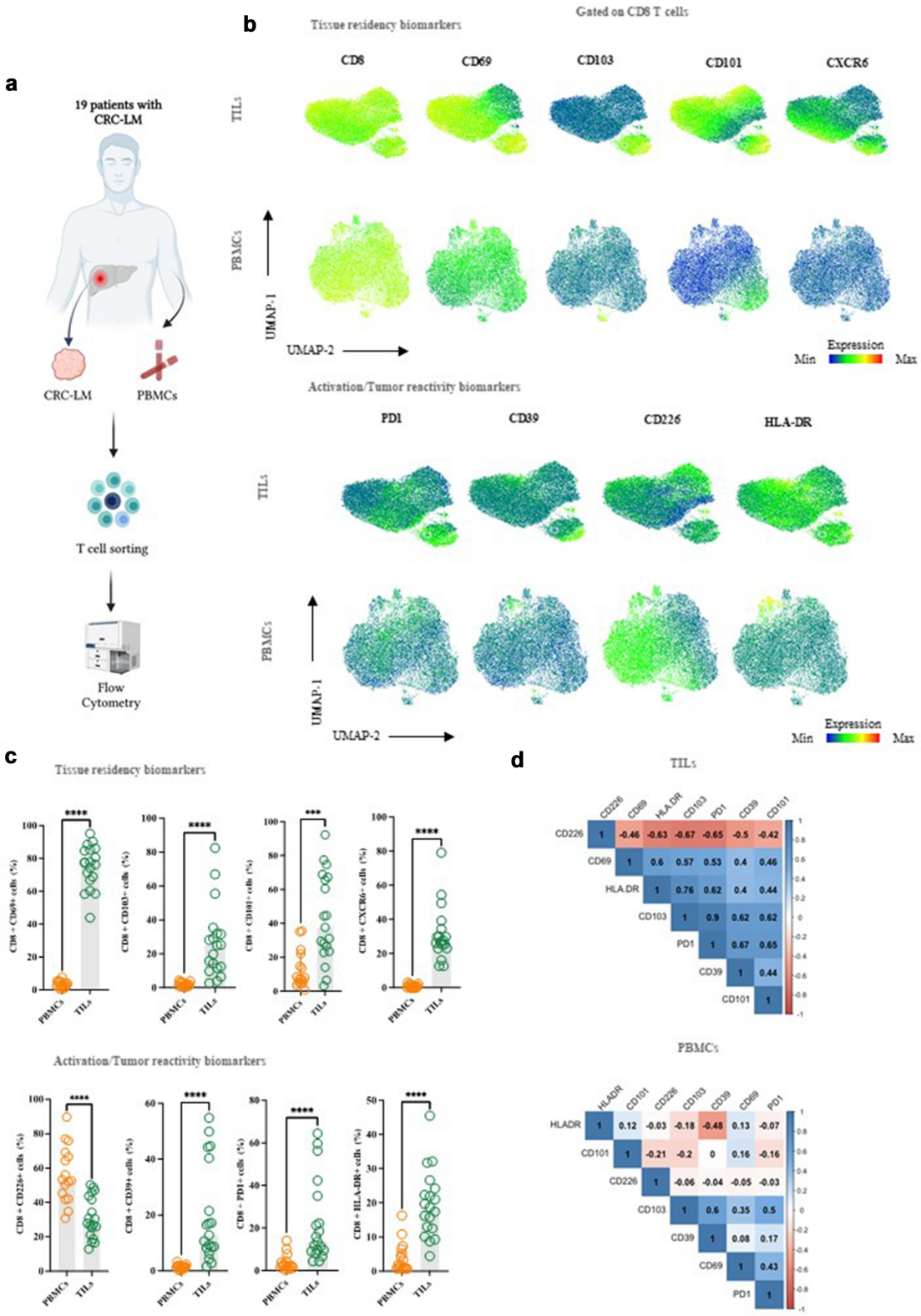

Figure 1. Phenotypic characterization of CD8$^+$ TILs and PBMCs in CRC liver metastases. (a) Study overview. (b) UMAP visualization of tissue residency (CD69, CD103, CD101, CXCR6), activation (CD226, HLA-DR), and tumor reactivity (PD1, CD39) biomarkers on CD8$^+$ PBMCs ($n = 16$) and TILs ($n = 19$). UMAP visualization was conducted on total T cells (c) analysis of tissue residency (CD69, CD103, CD101, CXCR6), activation (CD226, HLA-DR), and tumor reactivity (PD1, CD39) biomarkers expression between CD8$^+$ PBMCs and TILs. (d) Correlation matrix of studied biomarkers (CD69, CD103, CD101, CD226, HLA-DR, PD1, CD39) on TILs and PBMCs, positive correlations are indicated in blue, negative correlations are in red, $p < 0.05$ was considered significant. Statistical differences between the two groups were determined using the Mann–Whitney U test (c). *$p < 0.05$, **$p < 0.01$, ***$p < 0.001$, ****$p < 0.0001$.

metastases compared to circulating $CD8^+$ T cells, in line with a possible influence of TGF-β1 as we previously reported.[24] Interestingly, we also observed a correlation between CD69 and tissue residency biomarkers (Pearson's correlation coefficient, CD103 $r = 0.57$, CXCR6 $r = 0.5$ and CD101 $r = 0.46$, Figure 1d) along with activation/tumor reactivity biomarkers (Pearson's correlation coefficient, HLA-DR $r = 0.6$, PD-1 r = 0.53 and CD39 $r = 0.4$, Figure 1d). Collectively, these results indicate that CRC liver metastases $CD8^+$ TILs display a unique profile significantly different from circulating $CD8^+$ T cells, consistent with the reported tissue-resident memory T cells phenotype.

CD103 and CD69 residency molecules identify two distinct subsets of tissue-resident CD8 T cells enriched in CRC liver metastases

CD69 and CD103 expression have been widely used as tissue residency bona fide biomarkers. Two major populations of $CD8^+$ T_{RM} cells have been well validated on the phenotypic and transcriptional level: $CD103^-$ $^{CD69+}$ and $CD103^+CD69^+$.[14,15,19,28,29] Although the use of CD69 as a residency biomarker was highly questioned due to its expression on circulating activated T cells, it is now well-validated that $CD69^+$ TILs present a core residency program.[18] Nevertheless, recent studies demonstrated that T_{RM} cells display inter and intra-organ heterogeneity. A distribution analysis of several tissue residency biomarkers was conducted to explore this heterogeneity in CRC liver metastases. Following flow cytometry and UMAP analysis, two clusters expressing tissue residency biomarkers were identified as $CD103^-$ $CD69^+$ and $CD103^+CD69^+$(Figure 2a, b). Almost half of the tested CRC liver metastases $CD8^+$ TILs were $CD103^-$ $CD69^+$ (Median, 46.6%, 10.7%-81.7%) and roughly one-quarter co-expressed CD69 and CD103 (Median, 24.6%, 4%-84.2%) (Figure 2c). Both $CD103^-$ $CD69^+$and $CD103^+$ $CD69^+$ $CD8^+$ TILs showed significantly higher expression of tissue residency/activation biomarkers CXCR6, CD101, and HLA-DR compared to $CD103^-CD69^-CD8^+$ TILs, suggesting that both $CD103^-CD69^+$ and $CD103^+CD69^+$ represented two distinct T_{RM} subsets while $CD103^-CD69^-$ lack residency phenotype (Figure 2d). $CD103^-$ $CD69^+$ and $CD103^+CD69^+$ subsets showed distinct profiles regarding the expression of tissue residency/activation biomarkers. $CD103^+CD69^+$ subset showed significantly higher expression of CD101 as well as activation marker HLA-DR compared to $CD103^-CD69^+$ (Figure 2d). Interestingly, the correlation profile between the studied biomarkers differed between T_{RM} and non-T_{RM} cells and even between the two identified T_{RM} subsets (Figure 2e). Although PD-1 was correlated to CD39, HLA-DR as well as CD101 in the $CD103^+CD69^+$ subset, no correlation between PD-1 expression and CD39 nor HLA-DR was observed in the $CD103^-CD69^+$ T_{RM} subset (Figure 2e). This first set of experiments showed that different CD8 T_{RM} subsets infiltrate the tumor microenvironment of CRC liver metastases.

Tissue-resident $CD8^+$ T cells in colorectal cancer liver metastases exhibit higher cytotoxicity

T_{RM} cells were reported to be endowed with higher functionality compared to non-T_{RM} cells. To investigate T_{RM} cells functionality, *in vitro* activation of TILs was conducted. Interestingly, both T_{RM} populations ($CD103^+CD69^+$ and $CD103^-CD69^+$) presented higher production of IFNγ compared to non-T_{RM} cells ($CD103^-CD69^-$), whereas only $CD103^-CD69^+$ T_{RM} cells subsets reached statistical significance ($p = 0.0281$) (Figure 3a,b). Additionally, only $CD103^-$ $CD69^+$ T_{RM} cells presented higher production of TNFα (Figure 3a, b). Next, we investigated these T_{RM} cells polyfunctionality and capacity to produce more than one cytokine. $CD103^+$ $CD69^+$ and $CD103^-$ $CD69^+$ T_{RM} subsets presented slightly higher co-production of IFNγ and TNFα than non-T_{RM}, however, these data didn't research statistical significance (Figure 3c,d). Interestingly, both T_{RM} populations presented significantly higher production of GZMB compared to non-T_{RM} cells (Figure 3e). Similar results were observed for CD107a in degranulation assays, however, only $CD103^-CD69^+$ T_{RM} cells subsets reached statistical significance ($p = 0.0226$) (Figure 3e). All these observed data led us to speculate that T_{RM} cells seem to be more cytotoxic than non-T_{RM} cells.

$CD8^+$ $CD103^+$ $CD69^+$ T_{RM} cells display characteristics of tumor reactivity

PD-1 is an immune checkpoint also known as an antigen-experienced T cell marker. CD39 is a useful biomarker for distinguishing tumor-reactive T cells from bystander cells in the tumors.[16,19] To better discern tumor-reactive T_{RM} cells from bystanders, we sought to investigate the expression of these two markers in the identified T_{RM} subsets. $CD103^+$ $CD69^+$ T_{RM} cells showed significantly higher expression of PD-1 as well as CD39 compared to $CD103^-CD69^+$ T_{RM} subset (Figure 4a,b). On the other hand, non-T_{RM} cells showed very low expression of PD-1 and CD39. Interestingly, the majority of $CD103^+$ $CD69^+$ T_{RM} cells co-expressed PD-1 and CD39 suggesting a tumor-reactive T_{RM} population in CRC liver metastases (Figure 4c,d). Additionally, we investigated the gene expression of these tumor reactivity biomarkers in $CD103^+$ $CD69^+$ and $CD103^-CD69^+$ T_{RM} in GSE164522, which is a dataset of a single-cell RNA and TCR sequencing analyses comprising liver metastases of CRC. Same results were observed at the gene expression level, $CD103^+$ $CD69^+$ T_{RM} cells expressed higher levels of CD39 and PD-1 genes (ENTPD1 and PDCD1), along with CXCL13, a well-defined tumor reactive T cells biomarker[30] (Figure 4e-h).

$CD8^+$ $CD103^+$ $CD69^+$ T_{RM} cells are oligoclonal and exhibit a TCR repertoire distinct from the other TILs subsets

Next, we set out to investigate the TCR repertoire diversity of T_{RM} and non-T_{RM} cells. Therefore, the three TILs populations ($CD103^+CD69^+$, $CD103^-CD69^+$, $CD103^-CD69^-$) were sorted and bulk TCR sequencing was performed (Figure 5a). To assess the TCR repertoire diversity, CL50 (which represents the frequency of needed clonotypes to

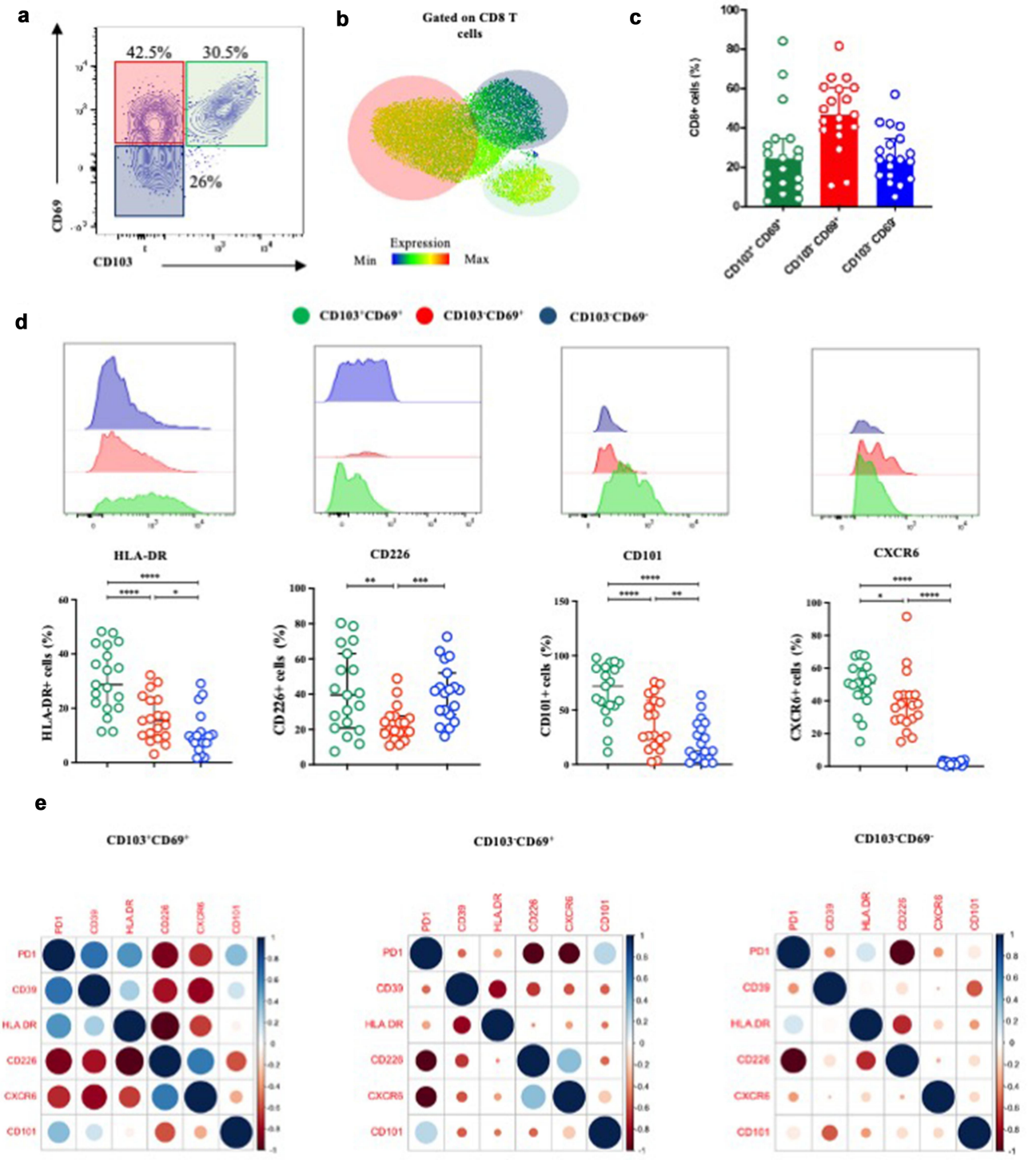

Figure 2. Phenotypic heterogeneity of CD8$^+$ T_{RM} subsets in CRC liver metastases. (a) FACS plots showing CD103 and CD69 expression on CD8$^+$ TILs, CD103$^-$CD69$^+$ T_{RM} cells are in red, CD103$^+$CD69$^+$ T_{RM} cells are in green, CD103$^-$CD69$^-$ non-T_{RM} cells are in blue. (b) UMAP visualization of the localization of the two T_{RM} (CD103$^-$CD69$^+$ T_{RM} in red and CD103$^+$CD69$^+$ T_{RM} in green) and the non-T_{RM} (CD103$^-$CD69$^-$ in blue) populations on CD8$^+$CD69$^+$ TILs. UMAP visualization was conducted on total T cells (c) frequency of T_{RM} (CD103$^-$CD69$^+$ in red and CD103$^+$CD69$^+$ in green) and non-T_{RM} cells (CD103$^-$CD69$^-$ in blue) in 19 patients with CRC liver metastases. (d) Expression analysis of tissue residency (CD101, CXCR6), and activation (CD226, HLA-DR) biomarkers between T_{RM} and non-T_{RM} cells. (e) Correlation matrix of CD101, CD226, HLA-DR, PD1, and CD39 expression on T_{RM} (CD103$^-$CD69$^+$ and CD103$^+$CD69$^+$) and non-T_{RM} (CD103$^-$CD69$^-$) cells, positive correlations are indicated in blue, negative correlations are in red. Statistical significance between three paired groups was assessed using one-way ANOVA with Tukey's multiple comparisons test (d), *$p < 0.05$, **$p < 0.01$, ***$p < 0.001$, ****$p < 0.0001$.

reach 50% of the TCR repertoire) was determined. CD103$^+$ CD69$^+$ T_{RM} population showed lower TCR repertoire diversity compared with CD103$^-$CD69$^+$ T_{RM} cells and non-T_{RM} cells, mirrored by a lower CL50 (Figure 5b,c). In fact, for CD103$^+$ CD69$^+$ T_{RM} only 2 to 8 expanded clonotypes were needed to reach 50% of the repertoire compared to 9 to 41 and 3 to 34 clonotypes for CD103$^-$CD69$^+$ T_{RM} cells and non-T_{RM} cells respectively (Figure 5b,c). We next

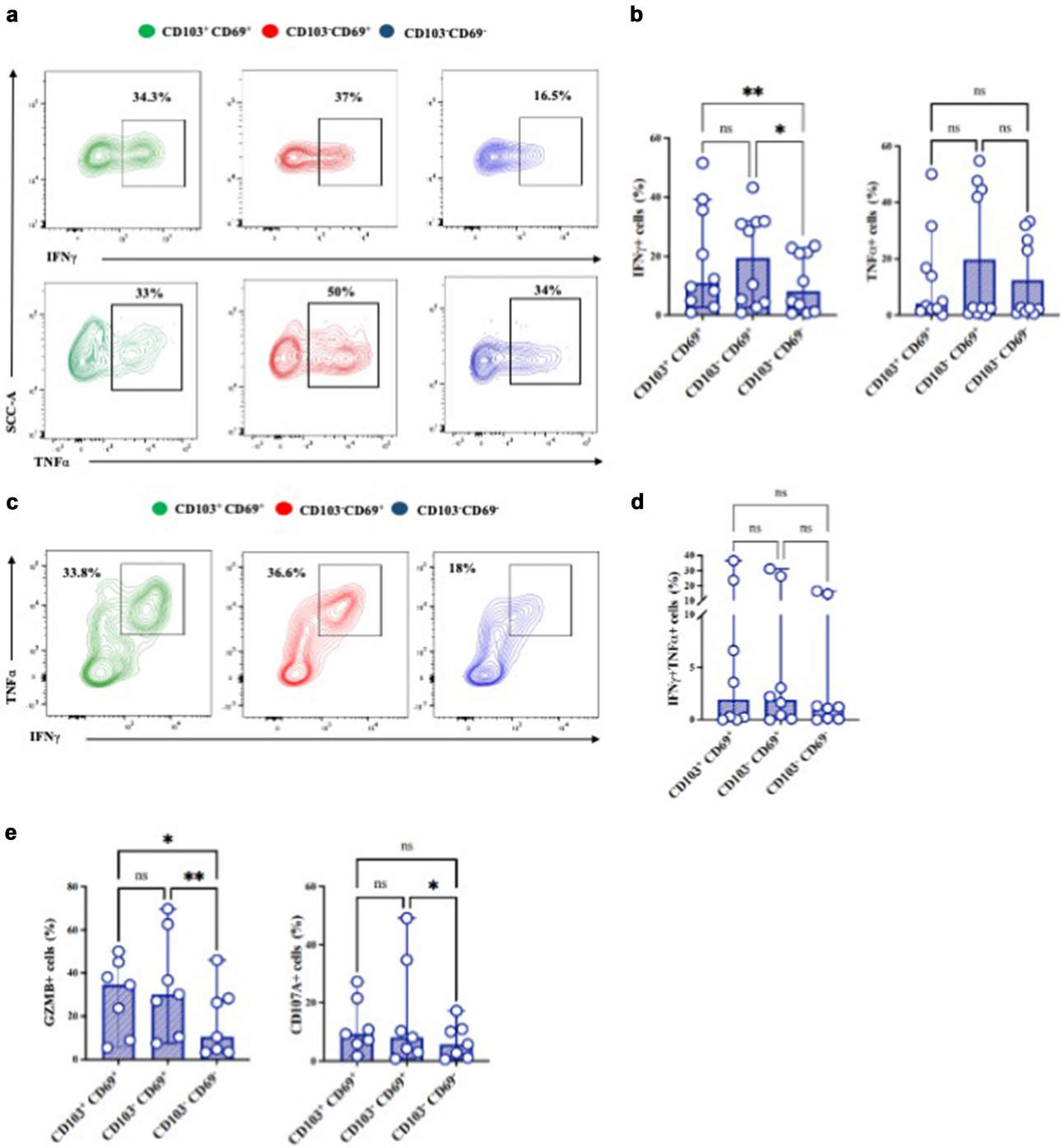

Figure 3. CD8$^+$ T_{RM} subsets in CRC liver metastases present an enhanced T cell function. (a) FACS contour plots showing IFNγ and TNFα production by T_{RM} and non-T_{RM} cells (b) comparison of IFNγ and TNFα production between T_{RM} and non-T_{RM} cells (c) FACS contour plots showing IFNγ and TNFα co-production by T_{RM} and non-T_{RM} cells (d) comparison of IFNγ and TNFα co-production by T_{RM} and non-T_{RM} cells. (e) Comparison of GZMB and CD107a production between T_{RM} and non-T_{RM} cells. Cells were activated with anti-CD3-CD28 stimulation for 5 hours. Statistical significance between three paired groups was assessed using one-way ANOVA with Tukey's multiple comparisons test, *$p < 0.05$, **$p < 0.01$, ***$p < 0.001$, ****$p < 0.0001$.

assessed whether the 5 most expanded clonotypes of CD103$^+$ CD69$^+$ T_{RM} cells are shared with other TILs populations. For the 5 tested patients, a total of 25 clonotypes were identified of which 13 (52%) were specific to the CD103$^+$ CD69$^+$ T_{RM} cells population (Figure 5d). Except for P2, overlap analysis showed the same tendency, with CD103$^+$ CD69$^+$ T_{RM} cells exhibiting a unique TCR repertoire (Figure 5e). Finally, analyses of the GSE164522 dataset of the single-cell TCR sequencing data revealed that the cluster C3 corresponding to CD103$^+$ CD69$^+$ T_{RM} cells showed higher number of clonally expander TCR compared to the other CD103$^-$ CD69$^+$ cells clusters (C1, C2, C4 and C5) (Figure 5f,g).

These data suggest that CD103$^+$ CD69$^+$ T_{RM} cells are more oligoclonal and exhibit a TCR repertoire distinct from the CD103$^-$ CD69$^+$ T_{RM} and non-T_{RM} subsets and therefore

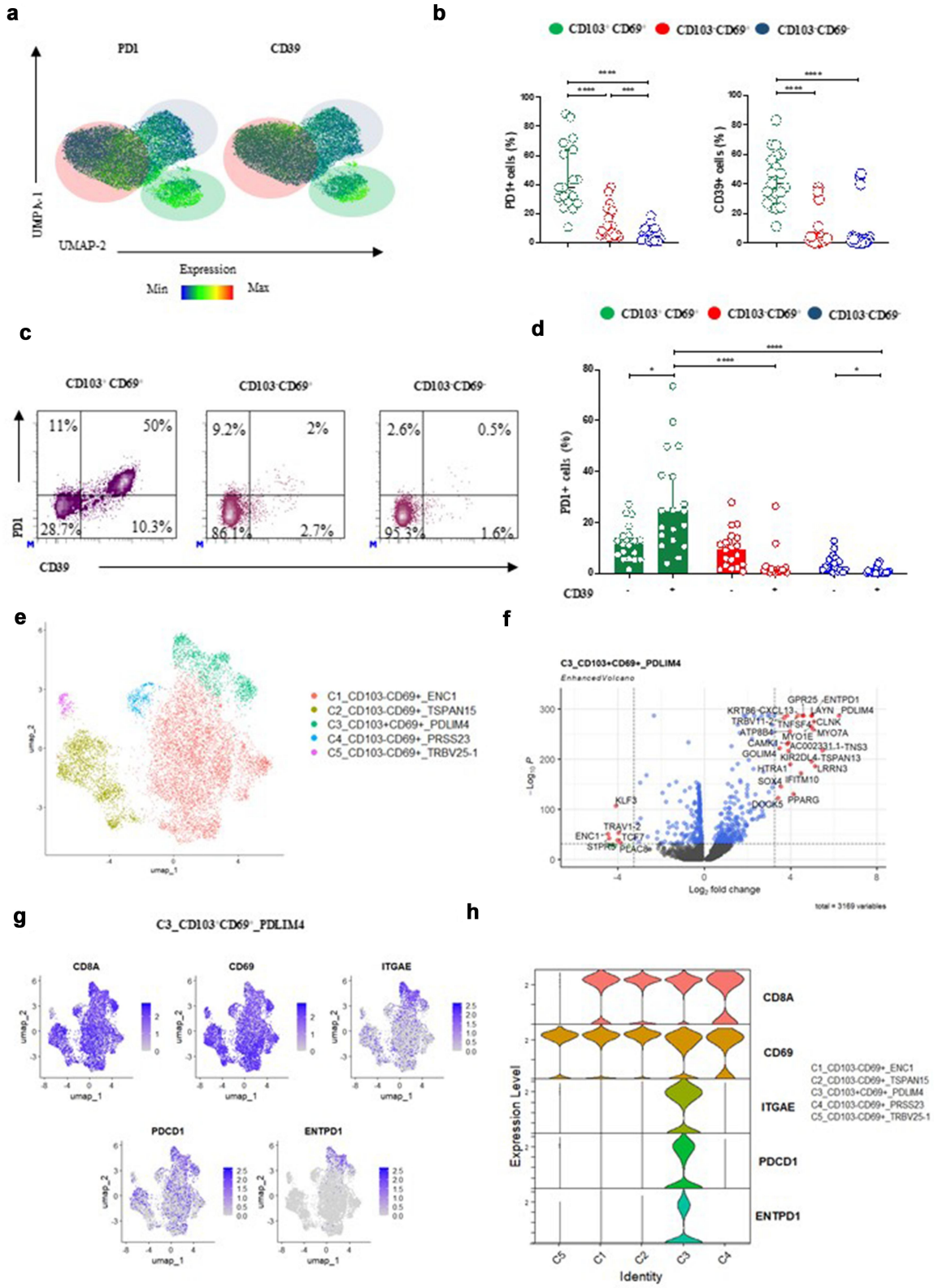

Figure 4. $CD8^+CD103^+CD69^+$ T_{RM} cells in CRC liver metastases are enriched in tumor reactivity biomarkers. (a) UMAP visualization of tumor reactivity (PD1, CD39) biomarkers on $CD8^+$ TILs ($n = 19$). UMAP visualization was conducted on total T cells (b) expression analysis of tumor reactivity (PD1, CD39) biomarkers between T_{RM} and non-T_{RM} cells. (c) FACS contour plots showing co-expression of PD1 and CD39 on T_{RM} and non-T_{RM} cells. (d) Analysis of co-expression of PD1 and CD39 between T_{RM} and non-T_{RM} cells. (e) Unsupervised clustering (UMAP plot) of scRnaseq data of TILs recovered from CRC liver metastases samples (GSE164522 dataset, $n = 17$ treatment-naïve patients), with key T cell subtypes annotated. (f) Volcano plot showing the most differentially expressed genes in the $CD8^+CD103^+CD69^+$ T_{RM} cells cluster (C3). (g) UMAP highlighting $CD8^+CD103^+CD69^+$ T_{RM} cells (cluster C3) and the expression of selected tumor reactivity genes PDCD1 and ENTPD1. (h) Violin plots showing the expression of selected tumor reactivity genes PDCD1 and ENTPD1 in different T_{RM} clusters. Statistical significance between three paired groups was assessed using one-way ANOVA with Tukey's multiple comparisons test, $^*p < 0.05$, $^{**}p < 0.01$, $^{***}p < 0.001$, $^{****}p < 0.0001$.

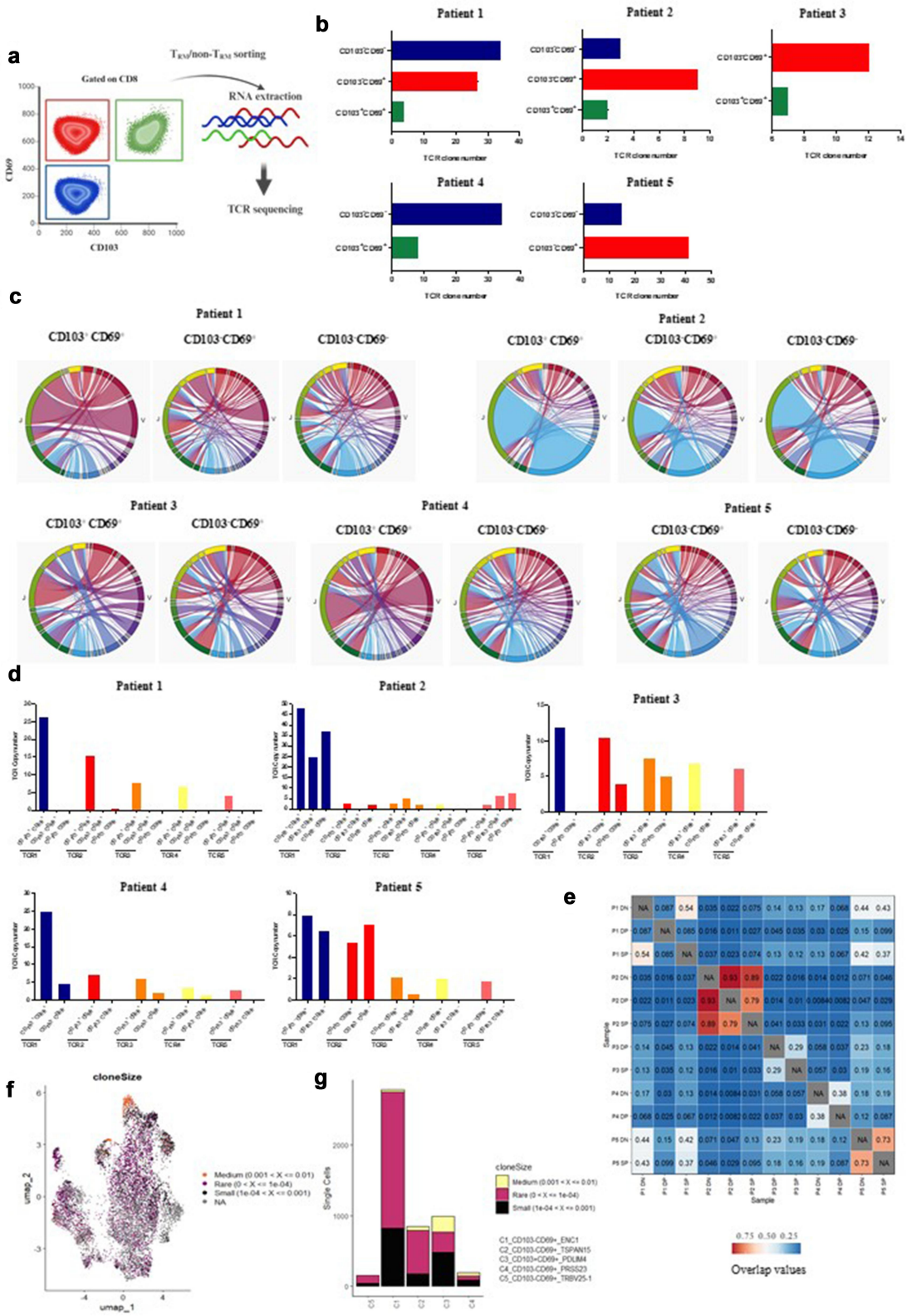

Figure 5. CD8$^+$CD103$^+$CD69$^+$ T_{RM} cells exhibit a distinct TCR repertoire in CRC liver metastases. (a) Sorting of T_{RM} and non-T_{RM} cells for TCRseq from 5 patients. (b) TCR repertoire diversity of T_{RM} and non-T_{RM} cells presented according to the CL50 defined as the frequency of needed clonotypes to reach 50% of the TCR repertoire.[23] clonotype was defined by the exact nucleotide CDR3 sequences of paired TCR α and β chains (c) circos plots showing the most expanded TCR in each T_{RM} and non-T_{RM} population (each chord represents a single TCR, the thickness of the chord is correlated to its expansion) (d) distribution of the 5 most expanded CD103$^+$CD69$^+$ T_{RM} cells clonotypes across CD103$^-$CD69$^+$ T_{RM} and CD103$^-$CD69$^-$ non-T_{RM} cells. (e) Clonal overlap (Morisita-Horn index) data of the TCRβ of all samples according to T_{RM} and non-T_{RM} populations. DP: CD103$^+$CD69$^+$ T_{RM} cells, SP: CD103$^-$CD69$^+$ T_{RM} cells, DN: CD103$^-$CD69$^-$ non-T_{RM} cells. (f) Unsupervised clustering (UMAP plot) of scTcrseq data of TILs recovered from CRC liver metastases samples (GSE164522 dataset, $n = 17$ treatment-naïve patients), showing the expanded TCRs. (G) Histogram showing the number of cells with clonally expanded TCRs in each cluster.

might represent the tumor-reactive T_{RM} population in the tumor microenvironment of CRC liver metastases.

CD8$^+$ CD103$^+$ CD69$^+$ T_{RM} subset express higher levels of CD49a

CD49a expression defines a distinct subset of T_{RM} cells in both normal skin and melanoma.[31,32] Expression of CD49a in T_{RM} derived from liver metastases was never delineated. To gain further insight into the phenotypic and functional characteristics of the two identified T_{RM} cells subsets in CRC liver metastases, we first determined the expression level of CD49a and then investigated whether it indicates a functional dichotomy. As previously described in other cancers, CD103$^+$CD69$^+$ and CD103$^-$ CD69$^+$ T_{RM} cells exhibited higher expression levels of CD49a compared to non-T_{RM} cells (Figure 6a). Notably, CD49a expression levels are enhanced in CD103$^+$ CD69$^+$ T_{RM} subset within CRC liver metastases compared to CD103$^-$ CD69$^+$ T_{RM}. A correlation between CD49a expression and PD-1 was observed in CD103$^+$ CD69$^+$ T_{RM} cells but not in CD103$^-$ CD69$^+$ T_{RM} cells (Pearson's correlation coefficient, $r = 0.62$, Figure 6b). CD49$^+$ and CD49$^-$ CD103$^+$ CD69$^+$ T_{RM} derived from liver metastases produced similar levels of IFNγ and TNFα (Figure 6c). CD49$^+$CD103$^-$CD69$^+$ T_{RM} cells on the other hand showed significantly higher production levels of INFγ (Figure 6d). On the other hand, the absence of PD1 and CD39 expression within CD49$^+$CD103$^-$CD69$^+$ T_{RM} suggests that CD49a does not contribute to the discrimination of a tumor-reactive population within CD103$^-$ CD69$^+$ T_{RM} cells.

By contrast to previous reports performed in melanoma and head and neck carcinoma, our results suggest that CD49a expression does not contribute to discriminating T_{RM} functions in CD103$^+$ CD69$^+$ TILs isolated from CRC liver metastases.

Infiltration of CRC liver metastases by CD8$^+$CD103$^+$CD69$^+$ T_{RM} is associated with improved patients' prognosis

Lastly, we investigated the prognostic value of T_{RM} cell populations in colorectal cancer liver metastases of 26 patients treated by surgery (Figure 7a). Dimensionality reduction analysis showed larger clusters of CD8$^+$ T_{RM} cells infiltration in patients who didn't present recurrence post-treatment of their liver metastases (Figure 7b). Additionally, tSNE analysis showed a more important presence of CD103$^+$CD69$^+$$T_{RM}$ cells in these patients, speculating a more infiltrated tumor microenvironment associated with a better prognosis (Figure 7b). To validate this hypothesis, statistical analyses were conducted based on flow cytometry data of T_{RM} classification into the previously identified two subsets and compared to total CD8 infiltration as well as infiltration by non-T_{RM} cells. Strikingly, neither total CD8 infiltration nor CD103$^-$CD69$^+$ levels were associated with CRC liver metastases patient's risk of relapse (Figure 7c). Only CD103$^+$CD69$^+$ T_{RM} cells presence was significantly associated

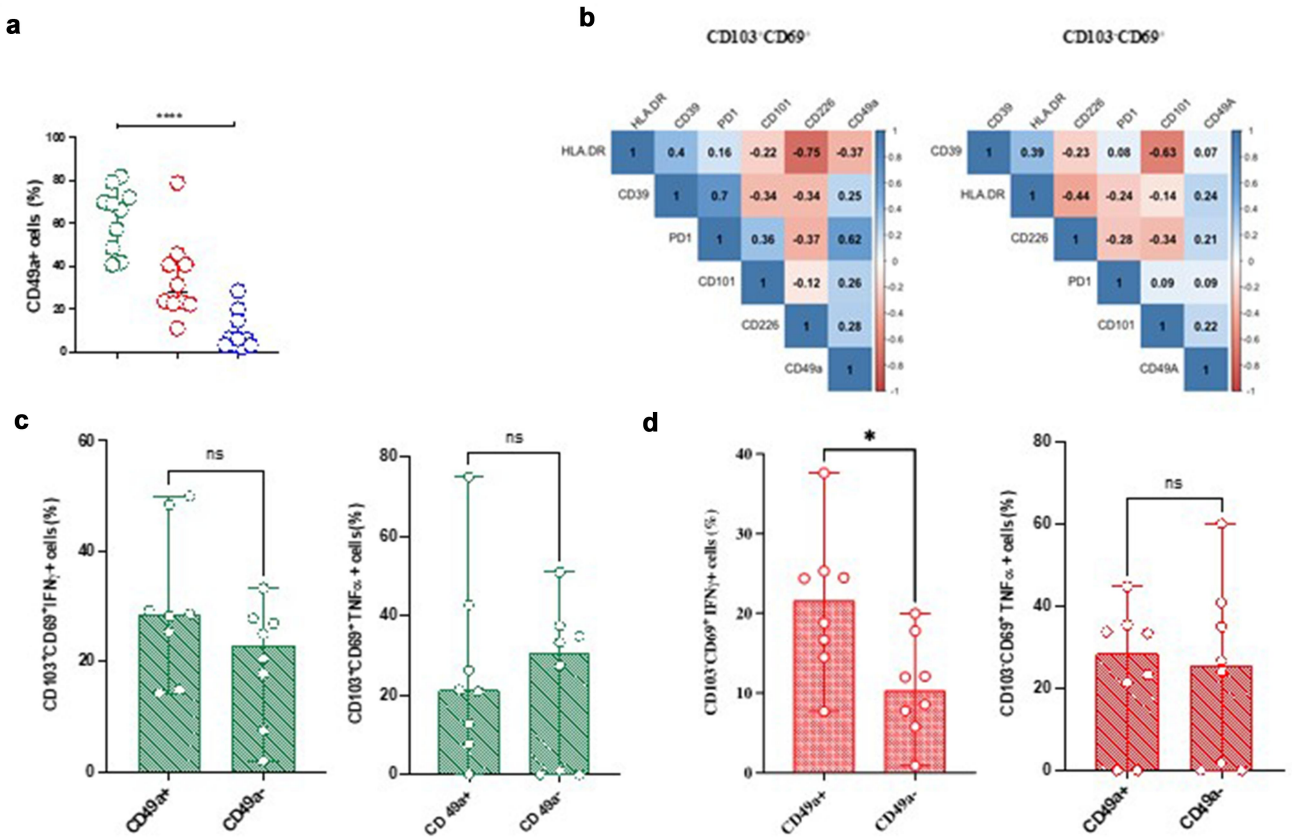

Figure 6. CD103$^+$ CD69$^+$ T_{RM} subset expresses higher levels of CD49a. (a) Analysis of CD49a expression between CD8$^+$ T_{RM} and non-T_{RM} cells. (b) Correlation matrix of HLA-DR, CD39, PD1, CD101, CD226, CD49a expression on CD103$^-$CD69$^+$ and CD103$^+$CD69$^+$ T_{RM} cells, positive correlations are indicated in blue, negative correlations are in red. (c) Comparison of IFNγ and TNFα production between CD103$^+$CD69$^+$CD49a$^+$ and CD103$^+$CD69$^+$ CD49a$^-$ T_{RM} cells (d) comparison of IFNγ and TNFα production between CD103$^-$CD69$^+$CD49a$^+$ and CD103$^-$CD69$^+$ CD49a$^-$ T_{RM} cells. Statistical differences between the two groups were determined using the Mann–Whitney U test. *$p < 0.05$.

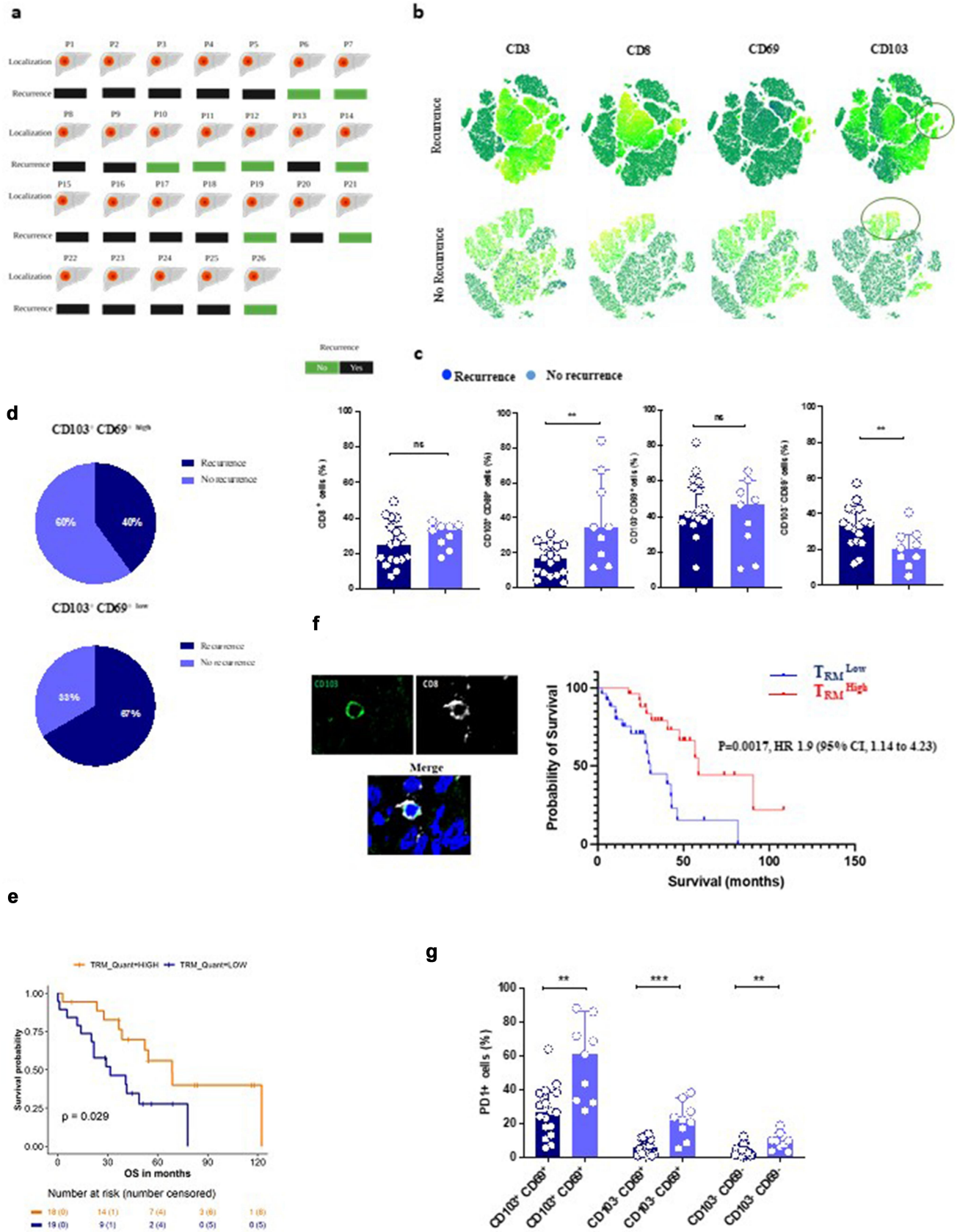

Figure 7. $CD103^{+}CD69^{+}$ T_{RM} cells associate with better outcome in CRC liver metastases. (a) Summary of patient's recurrence status ($n = 26$). (b) t-sne visualization of tissue residency biomarkers (CD69 and CD103) on $CD3^{+}CD8^{+}$ TILs ($n = 26$) according to recurrence status. t-sne visualization was conducted on total T cells (c) analysis of the expression level of different $CD8^{+}$ TILs populations according to recurrence status. (d). Distribution of $CD103^{+}CD69^{+}$ levels of expression according to recurrence status (e) Kaplan-Meier analysis of overall survival based on high and low expression levels of $CD103^{+}CD69^{+}$ T_{RM} cells using bulk RNAseq data. (f) Immunofluorescence staining of CD103 and CD8 on 52 TMA of CRC liver metastases and corresponding Kaplan-Meier analysis of overall survival based on high and low infiltration levels of $CD103^{+}CD69^{+}$ T_{RM} cells (g) analysis of PD1 expression across T_{RM} and non-T_{RM} subsets according to recurrence status. Statistical differences between the two groups were determined using the Mann–Whitney U test. Statistical significance between three paired groups was assessed using one-way ANOVA with Tukey's multiple comparisons test, $*p < 0.05$, $**p < 0.01$, $***p < 0.001$.

with a lower risk of relapse ($p = 0.0093$) (Figure 7c). Infiltration by non-T_{RM} cells was significantly associated with a higher risk of relapse ($p = 0.0110$) (Figure 7c). In line with these observations, 60% of patients with high $CD103^+CD69^+$ T_{RM} cells infiltration didn't relapse (Figure 7d). These results highlight the importance of $CD103^+CD69^+$ T_{RM} cells presence in CRC liver metastases patients' prognosis. To validate these data on the gene expression level, bulk RNA sequencing was conducted on 2 independent cohorts of over 30 patients with liver metastases. Noteworthy, $CD8^+CD103^+CD69^+$ gene signature was significantly associated with better overall survival of these patients (Figure 7e). Moreover, immunofluorescence conducted on 52 TMA samples of CRC liver metastases revealed that the density of total $CD8^+$ $CD103^+$ was also significantly correlated with better overall survival (Figure 7f). We then investigated the correlation of $CD103^+CD69^+$ T_{RM} cells with the clinicopathological features of CRC liver metastases (Table 1). Interestingly, the level of T_{RM} cells infiltration doesn't seem to be impacted by the classical clinicopathological features of CRC liver metastases such as age at diagnosis or pathological T stage nor associated with the total CD3 infiltration in metastases invasion margin (median of 1335 $CD3^+$ *vs* 1394 $CD3^+$, in T_{RM}^{high} and T_{RM}^{Low} respectively) or the tumor center (median of 197.8 $CD3^+$ *vs* 173.6 $CD3^+$, in T_{RM}^{high} and T_{RM}^{Low} respectively). Altogether, these data show that higher $CD103^+CD69^+$ T_{RM} infiltration seems to have an additive prognostic value to the conventional clinicopathological parameters. Finally, we sought to investigate the existence or not of a particular subpopulation of $CD103^+CD69^+$ T_{RM} cells associated with CRC liver metastases patients' prognosis. Only the expression of PD-1 allowed further stratification of the $CD103^+CD69^+$ T_{RM} subset associated with a lower risk of relapse (Figure 7g, supplementary data 1). These results showed that $CD103^+CD69^+$ T_{RM} cells are heterogeneous with different implications for patient outcomes.

Table 1. Clinicopathological parameters of colorectal cancer liver metastases patients according to $CD103^+CD69^+$ T_{RM} cells.

	T_{RM} $CD103^+CD69^{+\ High}$	T_{RM} $CD103^+CD69^{+\ Low}$
Age at diagnoses (years)		
Median	66.5	64
Range	52–75	53–75
Sex – n (%)		
Male	5(50)	11 (69)
Female	5(50)	5[31]
Location – n (%)		
Colon	7(70)	12(75)
Rectum	3[30]	4[25]
Location – n (%)		
Left	8(80)	15(94)
Right	2[20]	1[6]
Metastatic at diagnoses – n (%)		
Synchronous	6(60)	11(69)
Metachronous	4[18]	5[31]
Pathological T stage – n (%)		
T1	0	0
T2	0	1[6]
T3	7(70)	10(63)
T4	1[10]	4[25]
NA	2[20]	1[6]
Lymph node invasion – n (%)		
N0	2[20]	6[33]
N1	4[18]	5[31]
N2	2[20]	4[25]
NA	2[20]	1[6]
Microsatellite instability – n (%)		
MSI	0	0
MSS	9(90)	12(75)
Missing Value	1[10]	4[25]
RAS mutation – n (%)		
Yes	6(60)	10(63)
No	2[20]	4[25]
NA	2[20]	2[12]
RAF mutation – n (%)		
Yes	1[10]	1[6]
No	7(70)	13(81)
NA	2[20]	2[13]
$CD3^+$ T cells density in metastasis invasion margin		
Median (min-max)	1335 (348,[6] −2315)	1394(315,[6] −2621)
$CD3^+$ T cells density in metastasis tumor center		
Median (min-max)	197,8,[26] 09–1188)	173,6(86,[30] −722,0)
Chemotherapy before resection – n (%)		
Yes	6(60)	12(75)
No	4[18]	4[25]
Chemotherapy after resection – n (%)		
Yes	3[30]	10(63)
No	7(70)	6[34]

Discussion

Several studies have demonstrated the presence of T_{RM} cells in the tumor microenvironment of several solid tumors including primary liver and gastric cancers.[11] The presence of these cells was associated with improved outcome in these cancers. Interestingly, even though T_{RM} cells share one common core residency program, recent studies investigating the mechanisms of tissue residency establishment revealed a tissue-specific heterogeneity of T_{RM} cells that dictates their function and properties.[12] In this study, we speculated that the presence of T_{RM} cells in the tumoral immune infiltrate of colorectal cancer liver metastases could dictate these patient's prognosis.

In this work, using deep immunophenotyping, we established the phenotypic characteristics of $CD8^+$ T_{RM} cells in CRC liver metastases. We revealed the existence of two main T_{RM} cell subsets in liver metastases: $CD103^+CD69^+$ and $CD103^-CD69^+$ T_{RM} cells. These observations demonstrate the existence of an inter-tissue phenotypic heterogeneity of T_{RM} cells. Although it has been demonstrated that liver T_{RM} cells develop independently of TGF-ß signaling and therefore don't express CD103,[12] we found that one-quarter of the investigated T_{RM} cells in colorectal liver metastases expressed CD103. It is tempting to speculate that T_{RM} cells fate is dictated by the tumor microenvironment origin rather than the site of lodgment of T_{RM} cells itself as it has been previously reported.

Recent studies revealed that 80% of tumor antigen-specific and 90% of neoantigen-specific TILs are T_{RM} cells.[18,19] One of the most described biomarkers of tumor reactivity is CD39 expression whether it's on T_{RM} or non-T_{RM} cells.[16,35,36] Therefore, we used CD39 expression on CRC liver metastases T_{RM} subsets as a surrogate biomarker of tumor reactivity. Moreover, since PD-1 is also a well-established biomarker of antigen-experienced T cells,[37,38] its expression was also investigated. Interestingly, we noted an exclusive expression of both PD-1 and CD39 on the $CD103^+CD69^+$ T_{RM} cells subset. Moreover, we identified a striking correlation between PD-1 and CD39 expression on $CD103^+CD69^+$ T_{RM} cells. TCR sequencing data also showed that this population is more likely clonally expanded compared to $CD103^-CD69^+$ T_{RM} subset and non-T_{RM} cells. These interesting findings are consistent with the possibility that $CD8^+CD103^+CD69^+$ T_{RM} cells represent the tumor-reactive T cell population in CRC liver metastases. They are also consistent with a previous study in early breast cancer showing that tumor-specific T_{RM} cells are $CD103^+CD69^+$ and express CD39.[17]

Despite this observed phenotypic heterogeneity of T_{RM} cells in CRC liver metastases, it was not associated with a functional heterogeneity as previously reported in other cancers.[12,31,32] However, CRC liver metastases-derived T_{RM} cells showed higher INFγ production compared to non-T_{RM} cells, and $CD49a^+CD69^+CD103^+$ T_{RM} cells showed higher production levels of INFγ compared to $CD49a^+CD69^+CD103^-$ T_{RM} cells. This observation is in line with the findings of other studies that have demonstrated that T_{RM} cells exhibit higher functional and cytotoxic capacities compared to non-T_{RM} cells.[12,14,33,34] Noteworthy, despite the high expression of PD-1 by $CD103^+CD69^+$ T_{RM} cells, no sign of exhaustion was observed *in vitro*. since these cells showed high cytokine production similar to $CD103^-CD69^+$ T_{RM} cells. These findings support the hypothesis that PD-1 expression in T_{RM} cells is a hallmark of tissue residency program rather than T cell exhaustion.[14]

The presence of T_{RM} cells was reported to be associated with better patient prognosis in several cancers including gastrointestinal ones.[11,18,29] Of high importance is our finding that $CD103^+CD69^+$ T_{RM} presence but not $CD103^-CD69^+$ T_{RM} cells nor total CD8 infiltration is associated with better CRC liver metastases patients' outcome. Our Data were further supported by the positive association of the transcriptional profile of $CD103^+CD69^+$ T_{RM} cells with patients' overall survival. These findings highlight the fact that total CD8 infiltration may not be sufficient in terms of the patient's prognosis stratification. Although these observations need to be validated on a larger patient' cohort, it's tempting to speculate that the prognostic value of $CD103^+CD69^+$ T_{RM} cells in CRC liver metastases outperforms total CD8 one. The same results were reported by a recent study conducted on triple-negative breast cancer; analysis of the gene expression data of the METABRIC consortium showed that the T_{RM} signature had a superior prognostic value compared to CD8 and CD3 single gene expression.[39] Thus, quality and not only quantity matters when it comes to cancer elimination. In line with this, in contrast to the other T_{RM} and non-T_{RM} subsets, $CD103^+CD69^+$ T_{RM} cells displayed characteristics of tumor-reactive cells with the observed high expression of CD39 and the clonal expansion of their repertoire in CRC liver metastases. In line with our results, a recent single-cell analysis conducted on CRC liver metastases TILs showed the presence of a $CD8^+CXCL13^+$ population with high expression of CD103 and CD69 associated with better patient prognosis.[40]

This study has certain limitations. First, these findings should be validated on a larger TILs cohort of CRC liver metastases, especially regarding the investigation of the existence or not of a functional heterogeneity between T_{RM} subsets. Second, it would be interesting to validate the prognostic value of T_{RM} subsets on formalin-fixed tumor samples. Finally, to validate the tumor-reactive aspect of $CD103^+CD69^+$ T_{RM} cells, the establishment of a 3D organoid model or a co-culture of autologous tumor cells with the expanded $CD103^+CD69^+$ T_{RM} cells will help validate this observation.

In summary, our study demonstrates the existence of a phenotypic heterogeneity of T_{RM} cells in CRC liver metastases and allows the identification of a novel subpopulation of CD8 T_{RM} cells that expresses CD103 and CD69. This T_{RM} subset exhibited the characteristics of tumor reactivity as it expresses both PD-1 and CD39 and was correlated with better patients' prognosis. We conclude that $CD103^+CD69^+$ T_{RM} cells infiltration is considered a governing factor of CRC liver metastases patients' outcome with potential implication in optimal therapeutic strategies determination including immunotherapy administration for these cold tumors.

Acknowledgments

We would like to thank Tumorothèque de Franche Comté for providing tissue samples for this study and Mesocenter de calcul de Franche Comte for providing computational power for bioinformatics analysis. We Acknowledge funding from La Ligue Contre le Cancer.

Disclosure statement

No potential conflict of interest was reported by the author(s).

Funding

The work was supported by the Ligue Contre le Cancer.

Author contributions

Conceptualization: CB, SA. Methodology: FM, AB, EL, AEK, LS, AV, JRP, JV MK, AD, ZL, MBK. Writing original draft: SA, CB. Review and editing: CB, RL. Supervision: CB, RL. Funding acquisition: SA, CB, MK.

References

1. Urban SL, Jensen IJ, Shan Q, Pewe LL, Xue H-H, Badovinac VP, Harty JT. Peripherally induced brain tissue–resident memory CD8 + T cells mediate protection against CNS infection. Nat Immunol Nat Publishing Group. 2020;21(8):938–949. doi:10.1038/s41590-020-0711-8.
2. Szabo PA, Miron M, Farber DL. Location, location, location: tissue resident memory T cells in mice and humans. Sci Immunol. Vol. 4. American Association for the Advancement of Science; 2019. p. eaas9673.
3. Gueguen P, Metoikidou C, Dupic T, Lawand M, Goudot C, Baulande S, Lameiras S, Lantz O, Girard N, Seguin Givelet A, Lefevre M, Mora T, Walczak A, Waterfall J, Amigorena S. Contribution of resident and circulating precursors to tumor-infiltrating CD8+ T cell populations in lung cancer. Sci Immunol. 2021. p. eabd5778.
4. Amsen D, van Gisbergen Kpjm, Hombrink P, van Lier Raw, van Gisbergen KPJM, van Lier RAW. Tissue-resident memory T cells at the center of immunity to solid tumors. Nat Immunol. 2018;19 (6):538–546. doi:10.1038/s41590-018-0114-2.
5. Behr FM, Chuwonpad A, Stark R, Gisbergen Kpjm V. Armed and ready: transcriptional regulation of tissue-resident Memory CD8 T cells. Front Immunol. 2018;9:1770. doi:10.3389/fimmu.2018.01770.
6. Floc'h AL, Jalil A, Vergnon I, Chansac BLM, Lazar V, Bismuth G, Chouaib S, Mami-Chouaib F. αEβ7 integrin interaction with E-cadherin promotes antitumor CTL activity by triggering lytic granule polarization and exocytosis. J Exp Med. 2007;204 (3):559–570. doi:10.1084/jem.20061524.
7. Cepek KL, Shaw SK, Parker CM, Russell GJ, Morrow JS, Rimm DL, Brenner M. Adhesion between epithelial cells and T lymphocytes mediated by E-cadherin and the αEβ7 integrin. Vol. 372. 1994. 190–193.
8. Shiow LR, Rosen DB, Brdičková N, Xu Y, An J, Lanier LL, Cyster JG, Matloubian M. CD69 acts downstream of interferon-α/β to inhibit S1P1 and lymphocyte egress from lymphoid organs. 440. 2006. 540–544.
9. Cibrián D, Sánchez-Madrid F. CD69: from activation marker to metabolic gatekeeper. Eur J Immunol. 2017;47(6):946–953. doi:10.1002/eji.201646837.
10. Reilly EC, Lambert Emo K, Buckley PM, Reilly NS, Smith I, Chaves FA, Yang H, Oakes PW, Topham DJ. TRM integrins CD103 and CD49a differentially support adherence and motility after resolution of influenza virus infection. Proc Natl Acad Sci USA. 2020;117(22):12306–12314. doi:10.1073/pnas.1915681117.
11. Abdeljaoued S, Arfa S, Kroemer M, Ben Khelil M, Vienot A, Heyd B, Loyon R, Doussot A, Borg C. Tissue-resident memory T cells in gastrointestinal cancer immunology and immunotherapy: ready for prime time? J Immunother Cancer. 2022;10(4): e003472. doi:10.1136/jitc-2021-003472.
12. Christo SN, Evrard M, Park SL, Gandolfo LC, Burn TN, Fonseca R, Newman DM, Alexandre YO, Collins N, Zamudio NM, et al. Discrete tissue microenvironments instruct diversity in resident memory T cell function and plasticity. Nat Immunol. 2021;22 (9):1140–1151. doi:10.1038/s41590-021-01004-1.
13. Han J, Zhao Y, Shirai K, Molodtsov A, Kolling FW, Fisher JL, Zhang P, Yan S, Searles TG, Bader JM, et al. Resident and circulating memory T cells persist for years in melanoma patients with durable responses to immunotherapy. Nat Cancer. 2021;2 (3):300–311. doi:10.1038/s43018-021-00180-1.
14. Clarke J, Panwar B, Madrigal A, Singh D, Gujar R, Wood O, Chee SJ, Eschweiler S, King EV, Awad AS, Hanley CJ, McCann KJ, Bhattacharyya S, Woo E, Alzetani A, Seumois G, Thomas GJ, Ganesan AP, Friedmann PS, Elsner T, Ay F. Single-cell transcriptomic analysis of tissue-resident memory T cells in human lung cancer. J Exp Med. 2019;216(9):2128–2149. doi:10.1084/jem.20190249.
15. Savas P, Virassamy B, Ye C, Salim A, Mintoff CP, Caramia F, Salgado R, Byrne DJ, Teo ZL, Dushyanthen S, et al. Single-cell profiling of breast cancer T cells reveals a tissue-resident memory subset associated with improved prognosis. Nat Med Nat Publishing Group. 2018;24(7):986–993. doi:10.1038/s41591-018-0078-7.
16. Lee YJ, Kim JY, Jeon SH, Nam H, Jung JH, Jeon M, Soon Kim E, June Bae S, Ahn J, Yoo TK, Young Sun W, Gwe Ahn S, Jeong J, Park SH, Park WC, Kim S, Shin EC. CD39+ tissue-resident memory CD8+ T cells with a clonal overlap across compartments mediate antitumor immunity in breast cancer. Science immunology. Vol. 7. ; 2022. p. eabn8390.
17. Losurdo A, Scirgolea C, Alvisi G, Brummelman J, Errico V, Di Tommaso L, Pilipow K, Colombo FS, Fernandes B, Peano C, et al. Author correction: single-cell profiling defines the prognostic benefit of CD39high tissue resident memory CD8+ T cells in luminal-like breast cancer. Commun Biol. Nature Publishing Group. 2021;4(1):1–11. doi:10.1038/s42003-021-02789-5.
18. Cheng Y, Gunasegaran B, Singh HD, Dutertre C-A, Loh CY, Lim JQ, Crawford JC, Lee HK, Zhang X, Lee B, Becht E, Lim WJ, Yeong J, Chan CY, Chung A, Goh BKP, Chow PKH, Chan JKY, Ginhoux F, Tai D, Chen J. Non-terminally exhausted tumor-resident memory hbv-specific T cell responses correlate with relapse-free survival in hepatocellular carcinoma. Immunity. 2021;54(8):1825–1840.e7. doi:10.1016/j.immuni.2021.06.013.
19. Caushi JX, Zhang J, Ji Z, Vaghasia A, Zhang B, Hsiue E-C, Velculescu VE, Chaft JE, Kinzler KW, Zhou S, Vogelstein B, Taube JM, Hellmann MD, Brahmer JR, Merghoub T, Forde PM, Yegnasubramanian S, Ji H, Pardoll DM, Smith KN. Transcriptional programs of neoantigen-specific TIL in anti-PD-1-treated lung cancers. Vol. 596. Nature. Nature Publishing Group; 2021. p. 126–132.
20. Byrne A, Savas P, Sant S, Li R, Virassamy B, Luen SJ, Beavis PA, Mackay LK, Neeson PJ, Loi S, et al. Tissue-resident memory T cells in breast cancer control and immunotherapy responses. Nat Rev Clin Oncol. Nature. Publishing Group. 2020;17(6):341–348. doi:10.1038/s41571-020-0333-y.
21. Zhou H, Liu Z, Wang Y, Wen X, Amador EH, Yuan L, Ran X, Xiong L, Ran Y, Chen W, Wen Y. Colorectal liver metastasis: molecular mechanism and interventional therapy. Vol. 7. Sig Transduct Target Ther. Nature Publishing Group; 2022. p. 1–25.
22. Van den Eynde M, Mlecnik B, Bindea G, Fredriksen T, Church SE, Lafontaine L, Haicheur N, Marliot F, Angelova M, Vasaturo A, et al. The link between the multiverse of immune microenvironments in metastases and the survival of colorectal cancer patients. Cancer Cell. 2018;34(6):1012–1026.e3. doi:10.1016/j.ccell.2018.11.003.

23. Genolet R, Bobisse S, Chiffelle J, Arnaud M, Petremand R, Queiroz L, Michel A, Reichenbach P, Cesbron J, Auger A, et al. TCR sequencing and cloning methods for repertoire analysis and isolation of tumor-reactive TCRs. Cell Rep Methods. 2023;3 (4):100459. doi:10.1016/j.crmeth.2023.100459.
24. Viot J, Abdeljaoued S, Vienot A, Seffar E, Spehner L, Bouard A, Asgarov K, Pallandre J-R, Renaude E, Klajer E, et al. CD8+ CD226high T cells in liver metastases dictate the prognosis of colorectal cancer patients treated with chemotherapy and radical surgery. Cell Mol Immunol. Nature Publishing Group. 2023;20 (4):365–378. doi:10.1038/s41423-023-00978-2.
25. Liu Y, Zhang Q, Xing B, Luo N, Gao R, Yu K, Hu X, Bu Z, Peng J, Ren X, et al. Immune phenotypic linkage between colorectal cancer and liver metastasis. Cancer Cell. 2022;40(4):424–437.e5. doi:10.1016/j.ccell.2022.02.013.
26. Hao Y, Stuart T, Kowalski MH, Choudhary S, Hoffman P, Hartman A, Srivastava A, Molla G, Madad S, Fernandez-Granda C, et al. Dictionary learning for integrative, multimodal and scalable single-cell analysis. Nat Biotechnol. 2024;42(2):293–304. doi:10.1038/s41587-023-01767-y.
27. Borcherding N, Bormann NL. scRepertoire: an R-based toolkit for single-cell immune receptor analysis. F1000Res. 2020;9:47. doi:10.12688/f1000research.22139.1.
28. Kumar BV, Ma W, Miron M, Granot T, Guyer RS, Carpenter DJ, Senda T, Sun X, Ho S-H, Lerner H, et al. Human tissue-resident memory T cells are defined by core transcriptional and functional signatures in lymphoid and mucosal sites. Cell Rep. 2017;20 (12):2921–2934. doi:10.1016/j.celrep.2017.08.078.
29. Barsch M, Salié H, Schlaak AE, Zhang Z, Hess M, Mayer LS, Tauber C, Otto-Mora P, Ohtani T, Nilsson T, et al. T-cell exhaustion and residency dynamics inform clinical outcomes in hepatocellular carcinoma. J Hepatol Elsevier. 2022;77(2):397–409. doi:10.1016/j.jhep.2022.02.032.
30. Hanada K, Zhao C, Gil-Hoyos R, Gartner JJ, Chow-Parmer C, Lowery FJ, Krishna S, Prickett TD, Kivitz S, Parkhurst MR, et al. A phenotypic signature that identifies neoantigen-reactive T cells in fresh human lung cancers. Cancer Cell. 2022;40(5):479–493.e6. doi:10.1016/j.ccell.2022.03.012.
31. Zitti B, Hoffer E, Zheng W, Pandey RV, Schlums H, Perinetti Casoni G, Fusi I, Nguyen L, Kärner J, Kokkinou E, et al. Human skin-resident CD8+ T cells require RUNX2 and RUNX3 for induction of cytotoxicity and expression of the integrin CD49a. Immunity. 2023;56(6):1285–1302.e7. doi:10.1016/j.immuni.2023.05.003.
32. Cheuk S, Schlums H, Gallais Sérézal I, Martini E, Chiang SC, Marquardt N, Gibbs A, Detlofsson E, Introini A, Forkel M, et al. CD49a expression defines tissue-resident CD8 + T cells poised for cytotoxic function in human skin. Immunity. 2017;46(2):287–300. doi:10.1016/j.immuni.2017.01.009.
33. Hartana CA, Ahlén Bergman E, Broomé A, Berglund S, Johansson M, Alamdari F, Jakubczyk T, Huge Y, Aljabery F, Palmqvist K, et al. Tissue-resident memory T cells are epigenetically cytotoxic with signs of exhaustion in human urinary bladder cancer. Clin And Exp Immunol. 2018;194(1):39–53. doi:10.1111/cei.13183.
34. Kitakaze M, Uemura M, Hara T, Chijimatsu R, Motooka D, Hirai T, Konno M, Okuzaki D, Sekido Y, Hata T, et al. Cancer-specific tissue-resident memory T-cells express ZNF683 in colorectal cancer. Br J Cancer Nat Publishing Group. 2023;128 (10):1828–1837. doi:10.1038/s41416-023-02202-4.
35. Duhen T, Duhen R, Montler R, Moses J, Moudgil T, de Miranda NF, Goodall CP, Blair TC, Fox BA, McDermott JE, Chang SC, Grunkemeier G, Leidner R, Bell RB, Weinberg AD. Co-expression of CD39 and CD103 identifies tumor-reactive CD8 T cells in human solid tumors. 2018;9:2724.
36. Chow A, Uddin FZ, Liu M, Dobrin A, Nabet BY, Mangarin L, Lavin Y, Rizvi H, Tischfield SE, Quintanal-Villalonga A, et al. The ectonucleotidase CD39 identifies tumor-reactive CD8+ T cells predictive of immune checkpoint blockade efficacy in human lung cancer. Immunity. 2023;56(1):93–106.e6. doi:10.1016/j.immuni.2022.12.001.
37. Gros A, Robbins PF, Yao X, Li YF, Turcotte S, Tran E, Wunderlich JR, Mixon A, Farid S, Dudley ME, et al. PD-1 identifies the patient-specific $CD8^{+}$ tumor-reactive repertoire infiltrating human tumors. J Clin Invest Am Soc For Clin Investigation. 2014;124(5):2246–2259. doi:10.1172/JCI73639.
38. Kansy BA, Concha-Benavente F, Srivastava RM, Jie H-B, Shayan G, Lei Y, Moskovitz J, Moy J, Li J, Brandau S, et al. PD-1 status in CD8 + T cells associates with survival and anti-PD-1 Therapeutic outcomes in head and neck cancer. Cancer Res. 2017;77 (22):6353–6364. doi:10.1158/0008-5472.CAN-16-3167.
39. Savas P, Virassamy B, Ye C, Salim A, Mintoff CP, Caramia F, Salgado R, Byrne DJ, Teo ZL, Dushyanthen S, et al. Single-cell profiling of breast cancer T cells reveals a tissue-resident memory subset associated with improved prognosis. Nat Med. 2018;24 (7):986–993. doi:10.1038/s41591-018-0078-7.
40. Wang F, Long J, Li L, Wu Z-X, Da T-T, Wang X-Q, Huang C, Jiang Y-H, Yao X-Q, Ma H-Q, et al. Single-cell and spatial transcriptome analysis reveals the cellular heterogeneity of liver metastatic colorectal cancer. Sci Adv. 2023;9(24):eadf5464. doi:10.1126/sciadv.adf5464.